

## $m \times n$ Stacks of Discrete Aromatic Stacks in Solution

Yoshihiro Yamauchi,<sup>†</sup> Yuya Hanaoka,<sup>†</sup> Michito Yoshizawa,<sup>\*,†,§</sup> Munetaka Akita,<sup>‡</sup> Takahiro Ichikawa,<sup>||</sup> Masafumi Yoshio,<sup>||</sup> Takashi Kato,<sup>\*,||</sup> and Makoto Fujita<sup>\*,†</sup>

Department of Applied Chemistry, School of Engineering, The University of Tokyo, 7-3-1 Hongo, Bunkyo-ku, Tokyo 113-8656, Japan, Chemical Resources Laboratory, Tokyo Institute of Technology, 4259 Nagatsuta, Midori-ku, Yokohama 226-8503, Japan, PRESTO, Japan Science and Technology Agency (JST), and Department of Chemistry and Biotechnology, School of Engineering, The University of Tokyo, 7-3-1 Hongo, Bunkyo-ku, Tokyo 113-8656, Japan

Received April 15, 2010; E-mail: yoshizawa.m.ac@m.titech.ac.jp; kato@chiral.t.u-tokyo.ac.jp; mfujita@appchem.t.u-tokyo.ac.jp

**Abstract:** Septuple columnar stacks of large aromatic molecules with solubilizing side chains have been synthesized via one-step multicomponent self-assembly. At increased concentrations in aqueous solution,  $m \times n$  aggregates of aromatic stacks form. The simple addition of water induces lyotropic liquid-crystalline mesophases.

Columnar stacks of aromatic molecules can generate unique physical properties in molecular assemblies.<sup>1</sup> However, the number and variety of suitable stacking aromatics are rather limited, and alkyl side chains are often necessary to maintain column integrity and further increase the stacking number,  $n$ . Thus, the requisite ability to modulate the identity of the stacking unit and the value of  $n$  retards the engineering of specific properties into functional columnar-stacked aromatic systems such as discotic liquid crystals.<sup>2</sup> We previously demonstrated that discrete columns of aromatic stacks **1** can be assembled as interpenetrated coordination cages (Figure 1).<sup>3</sup> We thus envisioned that the columns of preformed aromatic stacks should also stack and generate extended stacks with a height of  $m \times n$  (where  $n$  is the number of stacks containing stacks of  $m$  aromatics) (Figure 1). Here, extended aggregates containing large numbers of stacked aromatics can quickly be generated, even when  $m$  or  $n$  is modest. Further modification is possible, as the intercalated aromatics and pillar subunits can be easily replaced.<sup>4</sup> We now report the formation of aggregates<sup>5</sup> of columnar stacks of  $m \times n$  aromatics in solution and in the solid state and also the generation of lyotropic liquid-crystalline mesophases.

In order to enhance cage<sup>6</sup> solubility and allow further structural elaboration, new pillar ligand **2b** was prepared from 3,6-di-4-pyridyl-1,2,4,5-tetrazine and dimethyl acetylenedicarboxylate via Diels–Alder and retro-Diels–Alder reactions in 80% yield.<sup>7</sup> The septuple aromatic stack **1b** quantitatively self-assembled after a suspension of pillar ligand **2b** (30  $\mu$ mol), tris(4-pyridyl)-2,4,6-triazine (**3**; 20  $\mu$ mol), and triphenylene (**5**; 60  $\mu$ mol) in a D<sub>2</sub>O solution (1.0 mL) of (en)Pd(NO<sub>3</sub>)<sub>2</sub> (**4**; 60  $\mu$ mol) was stirred at 40 °C for ~40 h. In the <sup>1</sup>H NMR spectrum (Figure 2), two sets of signals were observed for pillar **2b** ( $H_{a,b}$  and  $H_{a',b'}$ ), panel **3** ( $H_{d,e}$  and  $H_{d',e'}$ ), and guest **5** ( $H_{f,g}$  and  $H_{f',g'}$ ) in 1:1, 1:1, and 2:1 integral ratios, respectively. The stacked arrangement

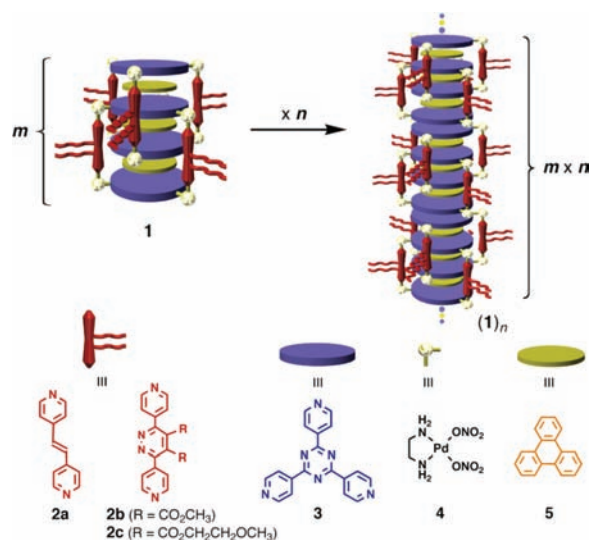


**Figure 1.** Schematic presentation of  $m \times n$  columnar stacks of stacks.

of panels **3** and guests **5** resulted in large upfield shifts ( $\Delta\delta = -1.1$  to  $-4.0$  ppm) and was indicative of encapsulation. Elemental analysis further supported the **2b**<sub>6</sub>·**3**<sub>4</sub>·**4**<sub>12</sub>·**5**<sub>3</sub> composition of **1b**.

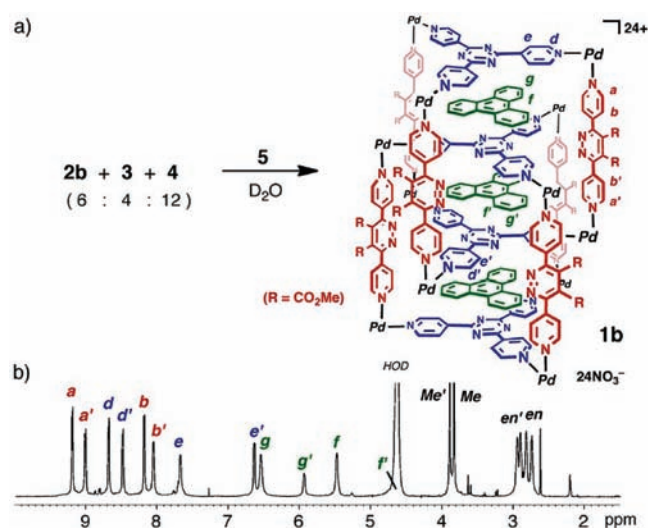


**Figure 2.** (a) Preparation of septuple aromatic stack **1b** by self-assembly from functionalized pillar ligand **2b**, panel ligand **3**, (en)Pd(NO<sub>3</sub>)<sub>2</sub> (**4**), and triphenylene (**5**). (b) <sup>1</sup>H NMR spectrum (500 MHz, D<sub>2</sub>O, 2.5 mM, 300 K) of **1b**.

<sup>†</sup> Department of Applied Chemistry, School of Engineering, The University of Tokyo.

<sup>‡</sup> Tokyo Institute of Technology.

<sup>§</sup> Japan Science and Technology Agency.

<sup>||</sup> Department of Chemistry and Biotechnology, School of Engineering, The University of Tokyo.

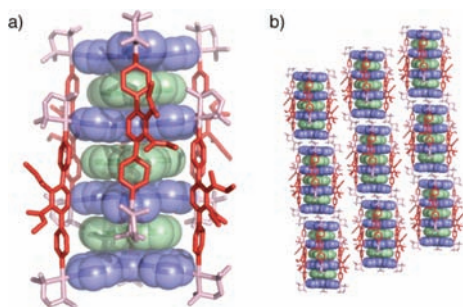


**Figure 3.** (a) X-ray crystal structure and (b) crystal packing of **1b'**.

Single crystals suitable for X-ray analysis were obtained by the slow concentration of an aqueous solution of **1b'** at room temperature for 1 week. **1b'** is an analogue of **1b** in which the ethylenediamine (en) on Pd(II) is replaced by the bulkier ligand *N,N,N',N'*-tetramethylethylenediamine (tmed).<sup>8</sup> The two cage sub-units of **1b'** are interlocked and establish three compartments, each accommodating a single triphenylene (**5**) (Figure 3). The seven aromatic molecules (four triazine panels and three triphenylene guests) stack at  $\sim 3.5$  Å intervals and generate a discrete, 2.4 nm long columnar stack. The molecular packing revealed ostensibly infinite columnar stacks, but closer inspection revealed that the bulky tmed “caps” hold neighboring columns  $\sim 6$  Å apart and effectively prohibit intermolecular aromatic interactions. In similar stacked structures,<sup>9</sup> intermolecular  $\pi$ - $\pi$  interactions between columnar cages were observed in the crystal when the smaller en caps were employed.

Because of the  $-\text{CO}_2\text{Me}$  groups on ligand **2b**, stack **1b** displayed increased water solubility, and at higher concentrations, aggregation was observed. At concentrations  $\leq 2.5$  mM, aqueous solutions of **1a** and **1b** both revealed a single band in the diffusion-ordered spectroscopy (DOSY) NMR spectrum with a diffusion coefficient ( $D$ ) of  $1.1 \times 10^{-10} \text{ m}^2 \text{ s}^{-1}$  (see the Supporting Information). Aqueous solutions of stack **1a** were saturated at  $\sim 4$  mM; however, at 10 mM, **1b** remained soluble and the diffusion coefficient decreased to  $6.3 \times 10^{-11} \text{ m}^2 \text{ s}^{-1}$ , suggesting the formation of aggregates. The  $^1\text{H}$  NMR signals of the external panel ligands ( $H_e$ ), intercalated aromatic molecules ( $H_g$ ,  $H_f$ ), and ethylenediamines on Pd(II) ions (*en*, *en'*) were broadened considerably (see the Supporting Information). However, at 10 mM, aqueous solutions of stack **1b'** (with bulky tmed groups) did not show similar aggregation behavior. Presumably, the steric bulk of the tmed cap effectively hides the exterior  $\pi$  surfaces and prevents intermolecular aromatic interactions. The glycol side chains of stack **1c** further increased the water solubility, and concentrations of up to 20 mM were achievable. At 20 mM, the  $^1\text{H}$  NMR signals also were broadened considerably (Figure 4), and the diffusion coefficient was further reduced to  $2.8 \times 10^{-11} \text{ m}^2 \text{ s}^{-1}$  as a result of increased aggregation (see the Supporting Information).

Under the assumption of cylindrical aggregation of column **1c**, the degree of aggregation ( $m$  and  $m \times n$ ) could be estimated using the diffusion coefficient and the Stokes–Einstein equation.<sup>10</sup> At 2.5 mM, the diffusion coefficient indicated a single  $\sim 3$  nm long stack, or  $n = 1$  and  $m \times n = 7$ . At 10 mM, the diffusion coefficient corresponded to a one-dimensional (1D) 12 nm long cylindrical aggregate, or  $n \approx 4$  and  $m \times n \approx 28$ .<sup>10,11</sup> At 20 mM, a 1D cylindrical aggregate would be 46 nm long, or  $n \approx 16$  and  $m \times n \approx 112$ . Bundled column aggregates are unlikely because hydrophobic and aromatic interactions between the top and bottom faces of **1b** and **1c**, rather than between the more hydrophilic glycol side

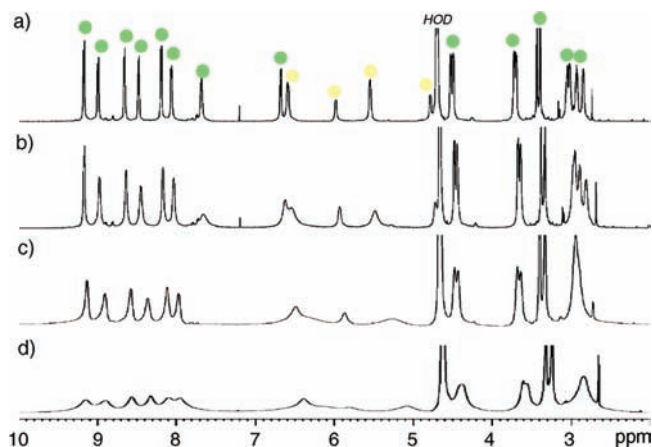


**Figure 4.** Concentration-dependent  $^1\text{H}$  NMR spectra (500 MHz,  $\text{D}_2\text{O}$ , 300 K) of **1c** at (a) 2.5, (b) 5.0, (c) 10.0, and (d) 20.0 mM. The spectra became broader as the concentration of **1c** was increased. Green circles indicate the host framework, and yellow circles indicate guest molecules.

chains, should be favored in aqueous solution. The lack of aggregate formation for **1b'** at 10 mM lends support to this interpretation.

When a minimal amount of water was added to dissolve compound **1c**, a viscous and turbid solution was obtained. The optical polarizing microscope texture of the solution (Figure 5) suggested that the solution forms a lyotropic nematic columnar ( $N_C$ ) phase having only 1D orientational order,<sup>12</sup> consistent with the proposed 1D columnar  $m \times n$  aggregates of **1c**. The apparent lack of two-dimensional order downplays significant side-chain interactions and likewise the presence of bundled aggregates.

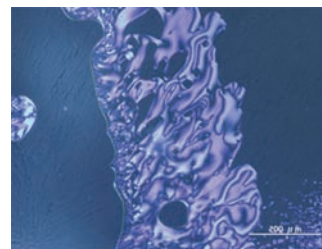


**Figure 5.** Optical polarizing microscope texture of **1c** in  $\text{H}_2\text{O}$ .

In summary, septuple columnar stacks **1** ( $m = 7$ ) of large aromatic molecules with solubilizing side chains were synthesized via one-step multicomponent self-assembly. At increased concentrations (10–20 mM) in aqueous solution, **1b** and **1c** formed  $m \times n$  aggregates of aromatic stacks via intermolecular hydrophobic and  $\pi$ - $\pi$  interactions with  $m = 7$  and  $n \approx 4$  and 16, respectively. In spite of the modest degree of aggregation, impressive  $m \times n$  values of  $\sim 28$  and  $\sim 112$  were achieved in water, underlining the potential utility of an  $m \times n$  approach. The simple addition of water induced lyotropic liquid-crystalline mesophases, promising potential application as a tunable liquid-crystalline material. Further structural control of the nascent material and physical properties is possible by simple modification of the pillar ligand (solubility and aggregation) or by choice of enclathrated aromatic guest (charge mobility, etc.).<sup>3,6</sup> Finally, we note that the  $m \times n$  assembly of aromatic stacks mimics hierarchical self-assembly found in nature, such as the arrangement of preassembled protein subunits into extended, functional biological superstructures.

**Acknowledgment.** This work was supported in part by KAKENHI (20111001 and 21108011). Y.Y. thanks JSPS for a Research Fellowship for Young Scientists.

**Supporting Information Available:** Experimental details, spectroscopic data, and crystallographic data (CIF). This material is available free of charge via the Internet at <http://pubs.acs.org>.

## References

- (1) (a) Kato, T.; Mizoshita, N.; Kishimoto, K. *Angew. Chem., Int. Ed.* **2006**, *45*, 38. (b) Laschat, S.; Baro, A.; Steinke, N.; Giesselmann, F.; Hägele, C.; Scalia, G.; Judele, R.; Kapatsina, E.; Sauer, S.; Schreivogel, A.; Tosoni, M. *Angew. Chem., Int. Ed.* **2007**, *46*, 4832.
- (2) (a) Adam, D.; Schuhmacher, P.; Simmerer, J.; Häussling, L.; Siemensmeyer, K.; Etzbach, K. H.; Ringsdorf, H.; Haarer, D. *Nature* **1994**, *371*, 141. (b) Bengs, H.; Closs, F.; Frey, T.; Funhoff, D.; Ringsdorf, H.; Siemensmeyer, K. *Liq. Cryst.* **1993**, *15*, 565. (c) Kato, T.; Matsuoka, T.; Nishii, M.; Kamikawa, Y.; Kanie, K.; Nishimura, T.; Yashima, E.; Ujiie, S. *Angew. Chem., Int. Ed.* **2004**, *43*, 1969. (d) Kumar, S. *Chem. Soc. Rev.* **2006**, *35*, 83. (e) Bisoyi, H. K.; Kumar, S. *Chem. Soc. Rev.* **2010**, *39*, 264.
- (3) Self-assembled discrete aromatic stacks: Klosterman, J. K.; Yamauchi, Y.; Fujita, M. *Chem. Soc. Rev.* **2009**, *38*, 1714.
- (4) Yamauchi, Y.; Yoshizawa, M.; Fujita, M. *J. Am. Chem. Soc.* **2008**, *130*, 5832.
- (5) (a) Sijbesma, R. P.; Beijer, F. H.; Brunsveld, L.; Folmer, B. J. B.; Hirschberg, J. H. K. K.; Lange, R. F. M.; Lowe, J. K. L.; Meijer, E. W. *Science* **1997**, *278*, 1601. (b) Yamaguchi, N.; Gibson, H. W. *Angew. Chem.* **1999**, *111*, 195; *Angew. Chem., Int. Ed.* **1999**, *38*, 143. (c) Takahashi, H.; Takashima, Y.; Yamaguchi, H.; Harada, A. *J. Org. Chem.* **2006**, *71*, 4878.
- (d) Fernández, G.; Pérez, E. M.; Sánchez, L.; Martín, N. *Angew. Chem., Int. Ed.* **2008**, *47*, 1094. (e) Yeboutchou, R. M.; Tancini, F.; Demitri, N.; Geremia, S.; Mendichi, R.; Dalcanale, E. *Angew. Chem., Int. Ed.* **2008**, *47*, 4504.
- (6) (a) Yoshizawa, M.; Nakagawa, J.; Kumazawa, K.; Nagao, M.; Kawano, M.; Ozeki, T.; Fujita, M. *Angew. Chem., Int. Ed.* **2005**, *44*, 1810. (b) Yamauchi, Y.; Yoshizawa, M.; Akita, M.; Fujita, M. *J. Am. Chem. Soc.* **2010**, *132*, 960.
- (7) Haddadin, M. J.; Firsan, S. J.; Nader, B. S. *J. Org. Chem.* **1979**, *44*, 629.
- (8) See the Supporting Information. Crystallographic data for **1b'** have been deposited at the Cambridge Crystallographic Data Centre (CCDC-759106).
- (9) See the following crystallographic data: CCDC-646911 and CCDC-703950.
- (10) Stokes–Einstein equation (cylinder model):

$$D = \frac{kT}{3\pi\eta L}(\ln p + v) \quad v = 0.312 + 0.565p^{-1} - 0.100p^{-2}$$

in which  $D$  is the diffusion coefficient,  $\eta$  is the solvent viscosity,  $k$  is the Boltzmann constant,  $T$  is the temperature,  $L$  is the cylinder length, and  $p = L/d$  is the axial ratio, where  $d$  is the cylinder diameter.

- (11) Wong, A.; Ida, R.; Spindler, L.; Wu, G. *J. Am. Chem. Soc.* **2005**, *127*, 6990.
- (12) A similar texture was observed for lyotropic liquid-crystalline solutions of folic acid derivatives exhibiting  $N_C$  phases: Kanie, K.; Yasuda, T.; Nishii, M.; Ujiie, S.; Kato, T. *Chem. Lett.* **2001**, 480.

JA103180Z